Supporting Information: Large and reconfigurable infrared photothermoelectric effect at oxide interfaces

Weitao Dai,[†, #] Yi Liang,[†, ‡, #] Ming Yang,[†] , Dustin Schrecongost,[†] Prakash Gajurel,[†] Hyungwoo Lee,[§] Jung-Woo Lee,[§] Chang-Beom Eom,[§] Cheng Cen[*,†]

[†]Department of Physics and Astronomy, West Virginia University, Morgantown, West Virginia 26506, USA

[‡]Guangxi Key Lab for Relativistic Astrophysics, Guangxi Colleges and Universities Key Lab of Novel Energy Materials and Related Technology, School of Physical Science and Technology, Guangxi University, Nanning, Guangxi 530004, China

[§]Department of Material Science and Engineering, University of Wisconsin-Madison, Madison, Wisconsin 53706, USA

*Corresponding author: cheng.cen@mail.wvu.edu

[#] These authors contributed equally to this work.

I： Experiments

The photovoltage was measured on a LAO/STO sample. 8 unit cells (uc) $LaAlO_3$ thin films were deposited on TiO_2 terminated (001) $SrTiO_3$ substrates via pulsed laser deposition (PLD) at 550°C under 10^{-3} mbar O_2 pressure. After deposition, the sample was cooled to room temperature under an oxygen pressure of 1 mbar. Ohmic contacts to the $LaAlO_3/SrTiO_3$ interface (enclosed by orange boxes in Figure 1(a)) were obtained as following: the electrodes were first patterned via optical lithography; 7nm depth of material was milled away in the electrode areas using Ar+ ion etching; etched areas were backfilled with 2nm Ti and 6nm Au by sputtering. For The metasurface absorber, the similar continuous film was fabricated by photolithography and maintains the electric connection to the $LaAlO_3/SrTiO_3$ interface. Then the cuboid array was fabricated at this film by

electron beam lithography (EBL) Then the metallic pads for wire bonding were fabricated by e-beam evaporation of 2nm Ti and 30nm Au on top of LAO surface. The e-beam evaporation structures (enclosed by the white dashed lines in Figure 1(a)) overlap partially with the ohmic contacts and the overlapped area is clearly visible in Figure 1(a).

After the fabrication of the metallic structures, the as-grown conductive interface of the 8 uc LAO/STO sample was insulted by oxygen plasma treatment. Then a Hall bar of conductive two-dimensional electron gas (2DEG) was created by conductive AFM lithography. Due to the damage of lead 2, an additional conductive channel was written between lead 2 and 5. The conductive 2DEG pattern was clearly imaged by Kelvin probe force microscope, as shown in the inset of Figure 1(a).

The sample was loaded to a cryostation from Montana Instruments and the scanning photovoltage microscope was performed with a continuous wave incident laser at a wavelength of 830nm through a home-made microscope system. The reflection signal (Figure 1(b)) was also monitored during the scan. The diameter of the focused laser point is estimated at 3μm based on the sharpness of the reflection images, which is close to the diffraction limit of the objective lens we used (20×, 0.25NA).

II：Optical absorption of nanocubroid metasurface

1. Introduction

Metasurfaces are ultrathin optical components which have many applications in optics and optoelectronics. Usually, they compose of artificially designed arrays of optical scatters. Here, we designed a good light metasurface absorber to optimize photovoltage generation and used finite element method (FEM) to simulate its photoabsorption.
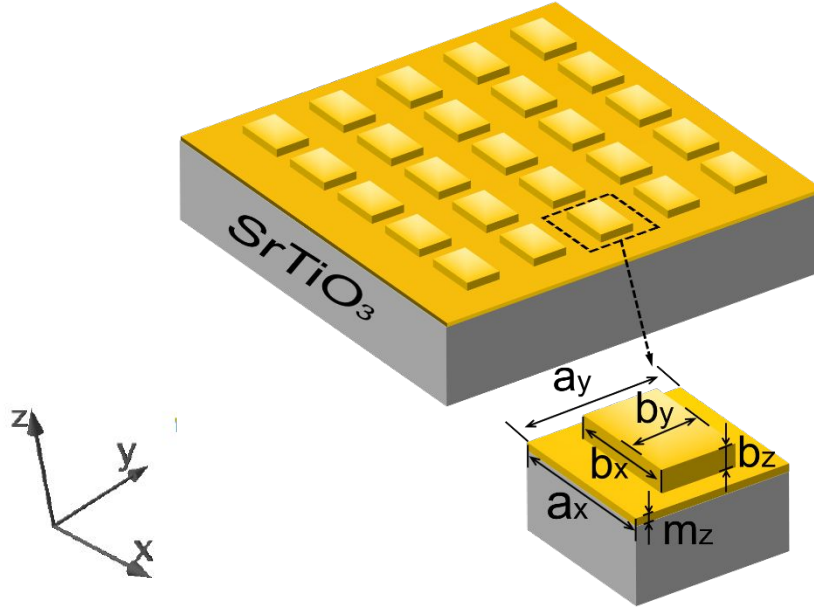
FIG. 1: Scheme of the device design. The blue area represents the $SrTiO_3$ substrate; the golden area represents the gold film with the gold cuboid array.

Figure 1 demonstrates the device design. The grey area represents the $SrTiO_3$ substrate. Since the $LaAlO_3$ layer was very thin and was removed in the area, we neglected it in the electromagnetic wave simulations. The golden area shows the gold nanostructures. Here we consider a simple design: a period nanocuboid array on a continue gold film. The continuous film can be fabricated by photolithography and maintains the electric connection to the $LaAlO_3/SrTiO_3$ interface. Then the cuboid array can be fabricated by one-step e-beam lithography. It is not easy to get high light absorption in the metal nanostructue from top-down approach due to the huge impedance mismatch between metal and air. The continuous film can only absorb 2.5% light at 800 nm. Metasurface absorber was invented to achieve perfect absorption by using two-layer metal metamaterials. But the absorption happens mainly in the dielectric layer between the two metal layers.

The coordinate system is also defined in Figure 1. The normal incident light comes from z direction and the electric field is along x direction. The nanostructure has six free parameters: the period along x and y direction a_x and a_y; the size of the top cuboids b_x, b_y and b_z; the thickness of the gold thin film m_z. We try to improve the absorption in the metal structure at 830 nm by tuning these six geometric parameters as below.
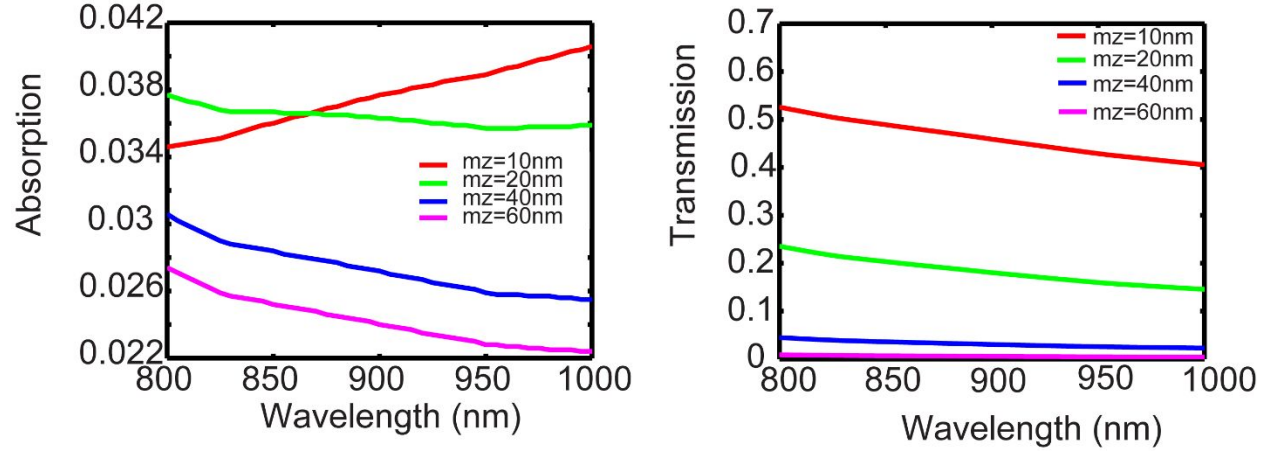
2. Device optimization

A. Continuous film

FIG. 2: The absorption and transmission of a continuous gold film on a SrTiO₃ substrate.

First, Figure 2 shows the absorption and transmission of a continuous gold film on a SrTiO$_3$ substrate. The absorption is around or less than 4% for various thicknesses. The transmission is not negligible when the film is thinner than 40 nm. We have to consider the reflection from the gold/SrTiO$_3$ interface and the interference effect. This explains the thinner film has higher absorption.
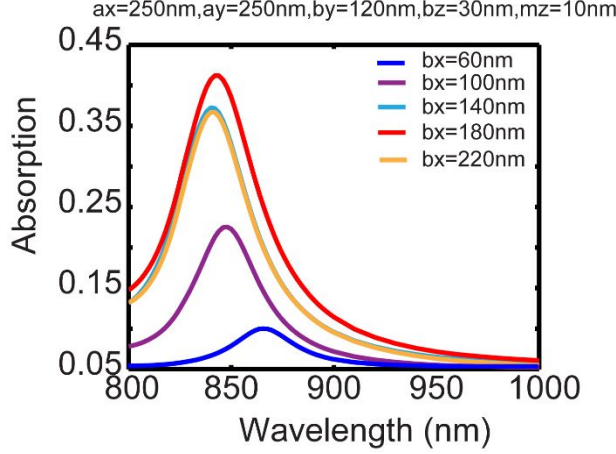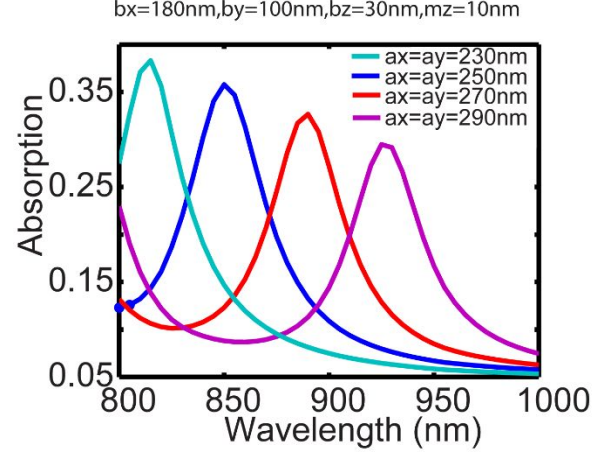
Fig.3: The absorption curves at various b_x Fig.4: The absorption curves at various a_x

B. Study of b_x

The simulation results of the absorption curves at various b_x are shown in Figure 3. The period of the structures is $a_x = a_y = 250$ nm, and b_x changes from 60 nm to a value close to the period. The period is chosen by considering the EBL capability and the size of the focused incident light. The focused light spot has diameter around 3μm and covers more than 10 periods of the nanostructure. So we can model the incident wave as a plane wave. The thickness of the bottom continuous film is $m_z = 10$ nm. In the actual devices, the continuous film contains a Ti film and an Au film, with total thickness around 10 nm. We will study the continuous film thickness later. The metal cuboid has thickness $b_z = 30$ nm.

From Figure 3, we found b_x not only change the absorption but also change the resonant wavelength for the largest absorption. However, when $b_x > 140$ nm, the wavelengths of the absorption peaks don't change much with b_x. Furthermore, one can see that b_x=180nm show the largest absorption peak, indicating that there is a best b_x for our metasurface absorber to realize largest absorption peak. It could not be too small or too large.

C. Study of a_x

Figure 4 demonstrates the absorption curves at various a_x. We can see clearly the peaks move with the period. The peaks move from 815 nm to 925 nm when the period changes from 230 nm to 290 nm. So, the parameter a_x decides the resonant wavelength for the largest absorption. When a_x increases, resonant wavelength move to larger value. Moreover, a_x is more important than b_x to tune the absorption peak to desired wavelength.
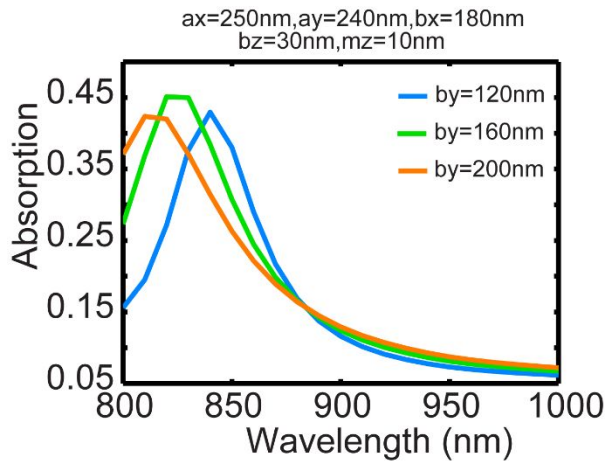

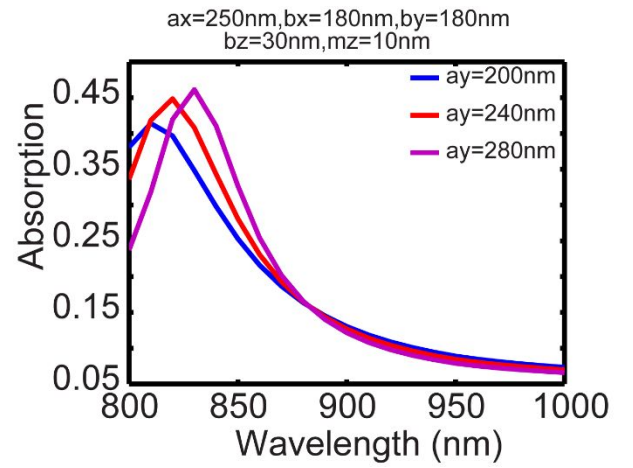Fig.5: The absorption curves at various b_y Fig.6: The absorption curves at various a_y

D. Study of a_y and b_y

Now we begin to study the geometry parameters along y direction: a_y and b_y. The rest parameters are: a_x = 250 nm, b_x = 180 nm, b_z = 30 nm and m_z = 10 nm. In Figure 5, a_y = 240 nm is fixed and b_y changes from 120 nm to 200 nm; in Figure 6, b_y = 180 nm is fixed and a_y changes from 200 nm to 280 nm. Both figures demonstrate the absorption spectra are also sensitive to the geometry parameters along y direction. When a_y is fixed, the peak wavelength moves to shorter wavelength when b_y increases, the same as Fig.3. When b_y is fixed, the peak wavelength moves to longer wavelength when a_y increases.

E. Optimization at λ= 830 nm

Figure 7 and 8 demonstrate the absorption of various nanostructures at λ= 830 nm. Figure 7 conveys similar messages as previous discussion: the absorption is sensitive to ax and not very sensitive to b_x. Next, we choose a_x = 250 nm, b_x = 170 nm, and study how a_y and b_y change the absorption in Figure 8. We found the absorption is sensitive to the difference between a_y and b_y; Clearly, when the difference is near 90nm, metasurface absorber shows the largest absorption. In this case we have multiply choices to achieve good absorption.
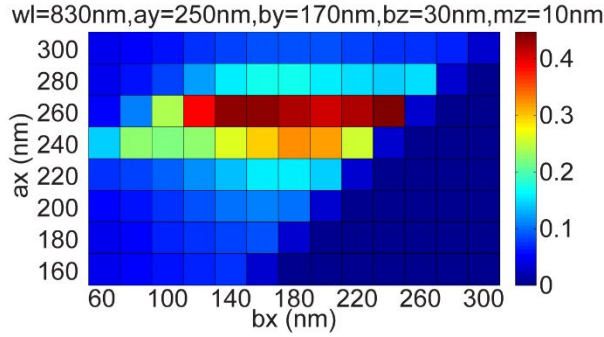

FIG. 7: Absorption at λ = 830 nm. a_y = 250 nm and b_y = 170 nm are fixed with various a_x and b_x combinations.
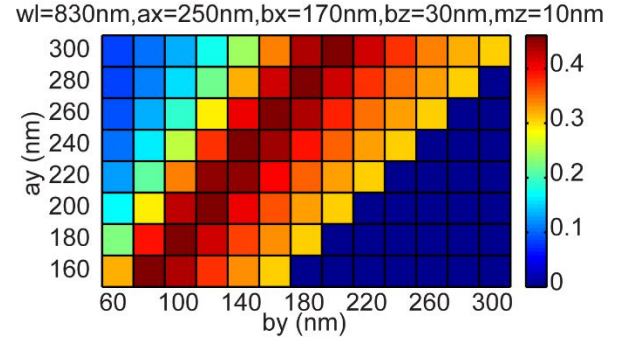

FIG. 8: Absorption at λ = 830 nm. a_x = 250 nm and b_x = 170 nm are fixed with various a_x and b_x combinations

F. Optimization of the thickness

Let's study the thickness of continuous film under the nanocuboid array first. Figure 8 demonstrates m_z is very important parameters. 2 nm increase of the thickness results significant change of the absorption spectra including the resonant wavelength and the absorption peak value. The absorption became weaker with the increasing thickness m_z. Actually, here, we have to consider

the coupling of the Au/SrTiO$_3$ interface and Au/air interface. The plasmonic modes supported by the thin metal film are very sensitive to the film thickness due to the coupling. So, the coupling from the Au/SrTiO$_3$ interface is crucial to get high absorption.

Next, we study the influence of b_z, the thickness of the cuboids. Figure 10 shows how the absorption spectra change with b_z at m_z=10nm. Generally, the larger the thickness, the larger the absorption. But the curves in the same figure have similar shapes and b_z cannot move the resonant wavelength a lot. The fact that the resonant wavelength is not very sensitive to the cuboid shape (b_x, b_y and b_z) suggests that the resonance comes from the plasmonic modes supported by the air/gold/SrTiO$_3$ multilayer structure and the cuboid array is used to excite the plasmonic modes.
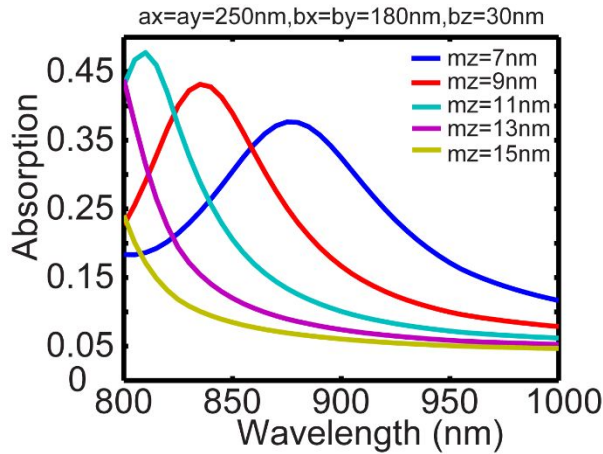

FIG. 9: Study of m_z, the thickness of continuous film under the nanocuboid array.
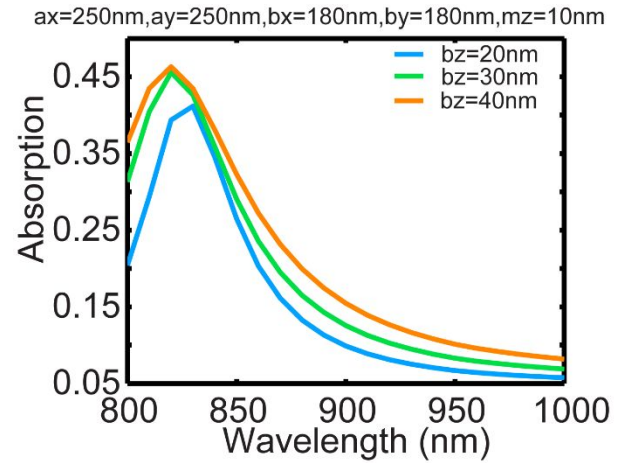
FIG. 10: Study of b_z, the thickness of the cuboids.

In conclusion, we have studied the influence of the six parameters of our metasurface absorber on photoabsorption via simulation. From these results, for our experiment, we can choose appropriate parameters to realize a strong absorption to improve photovoltage generation.